Research results from the Hohe Tauern Mountain Range - Permafrost/Rockfall Interaction at the Kitzsteinhorn & Proglacial Dynamics at the Obersulzbachkees

M. Geilhausen, I. Hartmeyer, H. Steyrer, L. Schrott

10TH ANNIVERSARY 15-20|SEPT SALZBURG

PANGEO AUSTRIA 2012

Exkursion 06
2012 - 09 - 19-20

TABLE OF CONTENTS

1. Geological setting / Geologische Situation - Hans Peter Steyrer

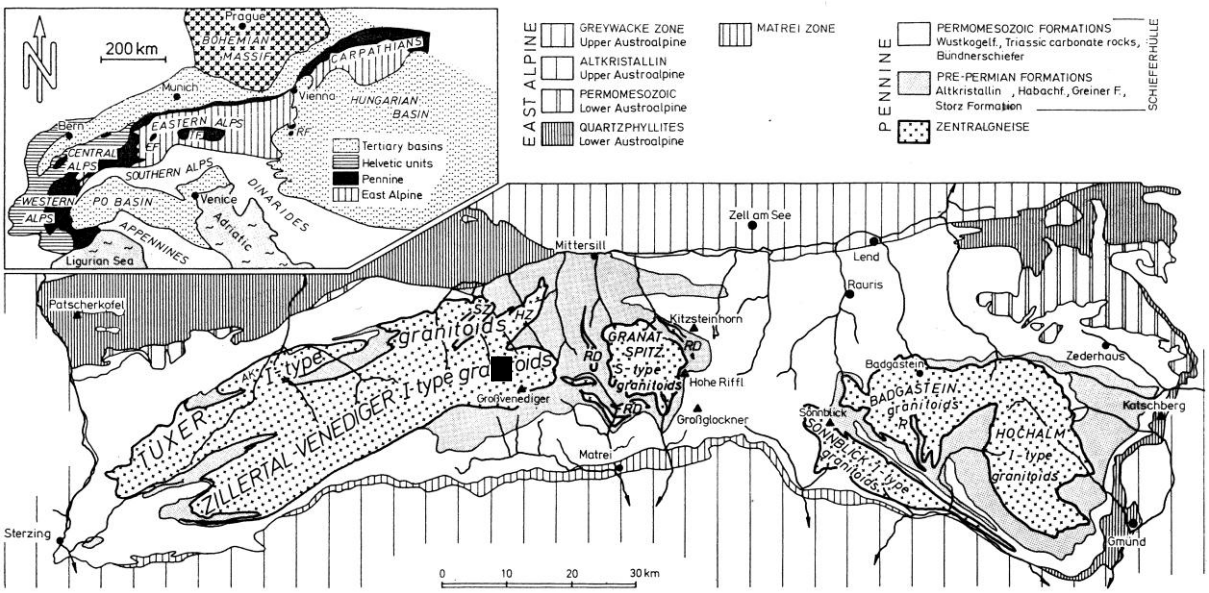

Fig. 1. - Geologische Übersichtskarte der Hohen Tauern mit den verschiedenen Zentralgneismassiven, -kernen und –decken (Finger et al. 1993, mit zahlreichen Referenzen)AK Ahorn Kern, GÖ Gößgraben Kern, HA Hochalm Ankogel Kern, HÖ Hölltor Rotgülden Kern, HZ Habachzunge, R Romate Decke, RD Riffldecke, SZ Sulzbachzungen Insert: EW Engadiner Fenster, RW Rechnitzer Fenster, S Schwarzwald, TW Tauernfenster, V Vogesen. Das Exkursionsgebiet im Obersulzbachtal ist durch das schwarze Rechteck gekennzeichnet.

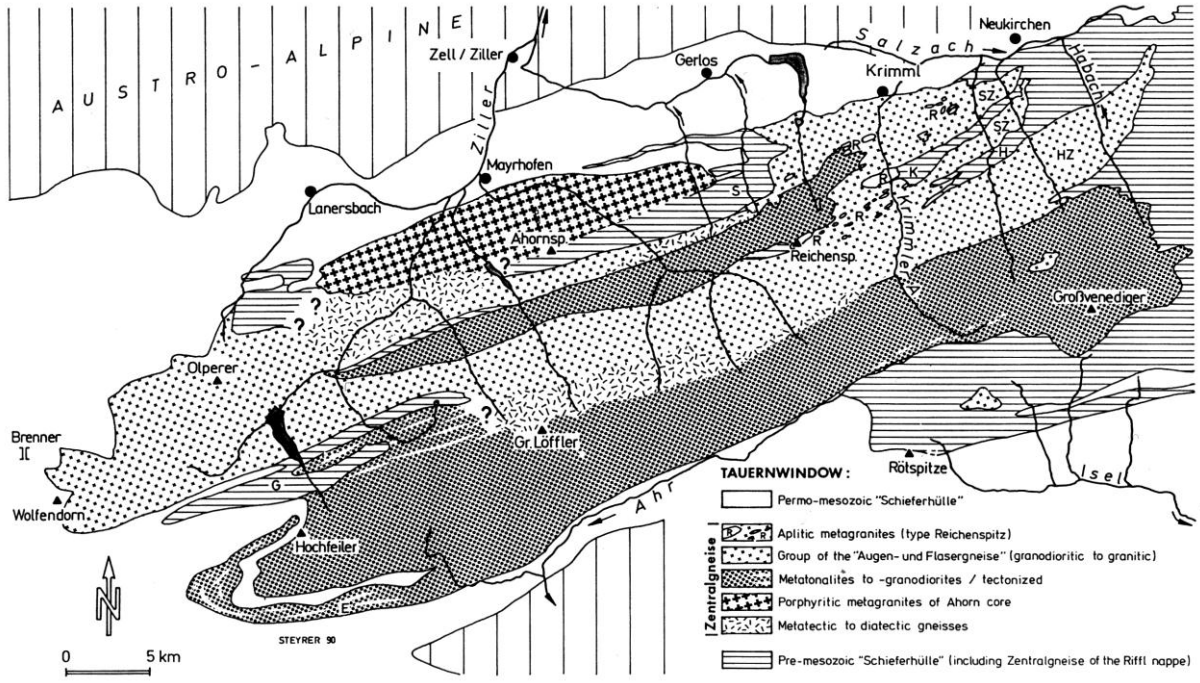

Fig. 2. - Geologische Karte des vormesozoischen Basements im westlichen Tauernfenster (Finger et al. 1993, mit zahlreichen Referenzen) mit dem Exkursionsgebiet (Rechteck südlich von Neukirchen). E Eisbrugglamelle, G Greiner Mulde, H Habachmulde, HZ Habachzunge, K Knappenwandmulde, R Granitgneise vom Typus Reichenspitz, S Schönachmulde, SZ Sulzbachzunge.

1.1. Der geologische Bau des Tauernfensters

Das Tauernfenster erstreckt sich vom Brennerpass im W bis zu Katschberg im E über eine Länge von etwa 160 km, und ist damit das bei weitem größte tektonische Fenster der Ostalpen. In ihm treten das Subpenninikum und das Penninikum unter den ostalpinen Decken zu Tage. Strukturell ist das Tauernfenster eine über 20 km mächtige Antiklinale, die in E-W Richtung walzenförmig in die Länge gezogen ist. Freigelegt wurde das Tauernfenster ab dem Miozän durch ein System von Abschiebungen und Seitenverschiebungen: die

Brennerabschiebung im W und die Katschbergabschiebung im E sind mächtige duktile Deformationszonen, die Salzachtalstörung am Nordrand und die Mölltalstörung am Südostrand des Tauernfensters sind die wichtigsten Seitenverschiebungen mit teilweise großer Vertikalkomponente. Diese bewirkt, dass heute zu beiden Seiten unterschiedliche Einheiten anzutreffen sind. Die von einer hohen älteren Metamorphose („Tauernkristallisation“) geprägten Einheiten des Fensterinneren grenzen an diesen Störungen an jünger überprägte, schwach metamorphe Decken des Ostalpins.

1.2. Geologischer Rahmen der Exkursion

Die spätpaläozoischen Zentralgneise – Ziel unserer Exkursion –sind Teil der Hohen Tauern, wo tiefe Einheiten des Alpinen Deckenstapels in einem tektonischen Fenster unter mächtigen Ostalpinen Deckenstapeln aufgeschlossen sind (Abb. 1) Etwa die halbe Fläche des Tauernfensters besteht aus permomesozoischen Einheiten, die andere Hälfte aus prä-permischen Gesteinen. Die Zentralgneise ihrerseits bilden etwa 2/3 der prä-permischen Gesteine. Die Zentralgneise sind meist in großen Antiformen aufgeschlossen, die im Bereich des Tauernfensters die tiefsten geologischen Einheiten bilden. Außer in den großen Kernen (Abb. 1) treten Zentralgneise auch in Form kleinerer Linsen oder Decken auf. Die Zentralgneise werden überwiegend von älteren Gesteinen umgeben, der sogenannten „Älteren Schieferhülle“. Die Kontakte zwischen den Zentralgneisen und der „Älteren Schieferhülle“ sind meist tektonisch überprägt und bevorzugte Lokalitäten für alpine Scherzonen. Andererseits liegen lokal permo-Trias oder Jura-Sedimente transgressiv auf den Zentralgneisen, was bedeutet, dass wenigstens Teile der Plutone bereits vor der Alpinen Orogenese freigelegt waren. Zusammen mit den übrigen Gesteinen des Tauernfensters wurden die Zentralgneise während der Alpinen Orogenese in Grünschiefer- bis Amphibolitfazies metamorph überprägt – daher auch das mehr oder weniger stark ausgeprägte Gneisgefüge, das oft kaum noch magmatische Reliktgefüge erkennen lässt.

1.3. Die Zentralgneise des Exkursionsgebietes

Das Exkursionsgebiet liegt in den westlichen Hohen Tauern, wo Zentralgneise in drei großen Kernen aufgeschlossen sind (Abb. 1 und Abb. 2): Ahorn Kern, Tuxer Kern und Zillertal Venediger Kern.
Das Obersulzbachtal liegt im Bereich des Zillertal-Venediger Kernes, der vom Tuxer Kern durch eine Störungszone getrennt ist. Der Zillertal-Venediger Kern besteht überwiegend aus mittelkörnigen Metatonaliten bis Metagranodioriten, die oft mit kleinen Körpern von Dioriten und Gabbros assoziiert sind. In den Zillertaler Alpen (Gebiet des Großen Löffler, Abb. 2.) sind die Tonalite und Granodiorite eng mit meta- und diatektischen Gneisen und Schollenmigmatiten assoziiert, während im Osten des Zillertal-Venediger Kernes die Kontakte zum Nebengestein zunehmend schärfer werden, was auf höhere Intrusionsniveaus schließen lässt. Im hinteren Krimmler Achental intrudieren die Tonalite in Kalifeldspat- und Biotit-reiche Anatexite und Augengneise, die am ehesten eine frühe Generation von Zentralgneisen darstellen (*Finger et al. 1993*).

2. Permafrost/Rockfall Interaction at the Kitzsteinhorn - Ingo Hartmeyer

The first day of the excursion primarily focuses on permafrost dynamics and permafrost-related processes in the Kitzsteinhorn summit region. Data and results presented have been achieved within the **research project MOREXPERT** ('Developing a Monitoring Expert System for Hazardous Rock Walls').

2.1. Motivation & Objectives of the MOREXPERT project

The stability of a permafrost-affected rock face is influenced significantly by its thermal state. Warming alters the (temperature-dependent) mechanical properties of joint surfaces and joint ice and therefore potentially causes temperature-related destabilization. Thus, particularly within the context of climate change instability of high-alpine rock faces is becoming an increasingly important risk factor for man and infrastructure (Mellor 1973, Davies et al. 2000, Krautblatter et al. 2010).

Numerous rock fall events in the European Alps (e.g. in the hot summers of 2003 and 2005) point to a possible increase of gravitational mass movements due to changing climate conditions (Gruber and Haeberli 2007). However, due to the lack of long-term data series on alpine permafrost conditions this assumption remains uncertain. The MOREXPERT project contributes to filling this gap by initiating a new long-term monitoring site focusing on permafrost and mass movement interaction at the Kitzsteinhorn (3.203 m), Hohe Tauern Range, Austria (Keuschnig et al. 2011).

Long-term data series on ground thermal conditions, comparable to meteorological data, are essential since permafrost distribution potentially responds very slowly to changing climatic conditions. For this reason the projects Permafrost and Climate in Europe (PACE) (Harris et al., 2001), the Swiss Permafrost Network (PERMOS) (Noetzli and Vonder Muehll 2010) and the Longterm Permafrost Monitoring Network (PermaNET) (Mair et al. 2011) have initiated long-term permafrost monitoring sites in the European Alps. Particularly high mountain peaks in the western European Alps (e.g. Schilthorn, Matterhorn, Aiguille du Midi) have been instrumented for continuous monitoring of permafrost (Gruber et al. 2004a, Ravanel et al. 2011). Prior to the establishment of the Kitzsteinhorn site extensive permafrost monitoring in Austria (deep boreholes, geophysics) was limited to one site, situated at Hoher Sonnblick (3.105 m) (Klee and Riedl 2011)

The main Objective of the MOREXPERT project is the development of a 'Best-Practice-Guide' for slope stability assessment in steep bedrock, which will consist of (i) a combination of the most appropriate methods and techniques, (ii) an assessment of required data and resolution, (iii) an efficient data analysis and documentation. The developed 'Best-Practice-Guide' is intended to significantly improve the risk management process for permafrost-related natural hazards in steep rock faces.

2.2. Study Area

The study area encompasses the entire summit region of the Kitzsteinhorn (3.203 m), covering approximately 3.5 ha and a vertical elevation difference of 300 m (fig. 3). The Kitzsteinhorn is located just north of the main

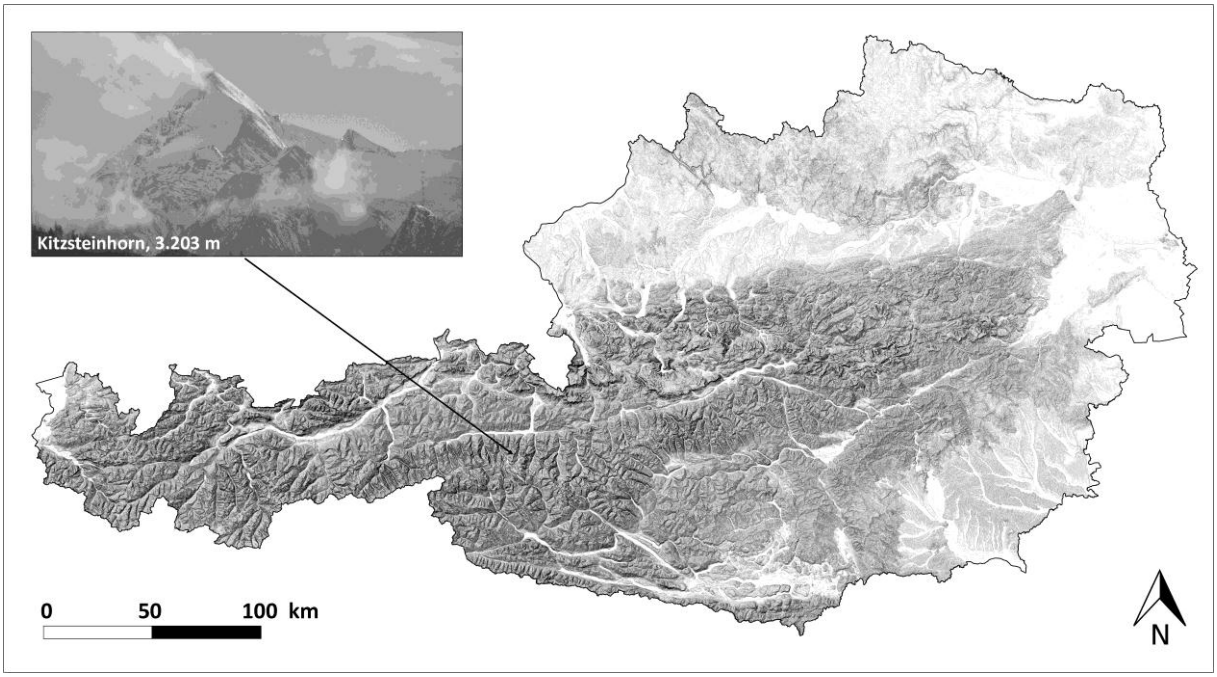

Fig. 3 - Location of the study area

Alpine divide and has no directly adjacent summits. In combination with its pronounced pyramidal shape these topographical features make the Kitzsteinhorn ideal for the investigation of the influence of aspect and elevation on ground thermal conditions. The small-scale lateral variability of ground thermal conditions in alpine terrain has contributed to the selection of a comparatively small study area.

The Kitzsteinhorn primarily consists of calcareous-micaschists. Stress release and intense physical weathering processes, typical for periglacial environments, resulted in the formation of an abundance of joint sets with large apertures. Intense retreat of the Schmiedingerkees glacier in recent decades led to the exposure of oversteepened rock faces, which in turn are frequently affected by minor rock fall events (Hartmeyer et al., 2012).

The tourism infrastructure existing within the study area (cable car, ski lifts, ski slopes etc.) provides easy access and enables convenient transportation of measuring equipment, an essential prerequisite for an extensive long-term monitoring program. The west ridge of the Kitzsteinhorn is tunneled by a gallery (‘Hanna-Stollen’), which allows the acquisition of thermal information from depths of up to 80 m below the terrain surface.

2.3. Methods / Monitoring Concept

Based on numerous preliminary investigations (permafrost modeling, ERT measurements, geomorphological & geotechnical surveys) a monitoring concept has been developed which is currently implemented. The monitoring system comprises various methods that allow the acquisition of (complementary) information on atmospheric, surface and subsurface conditions (fig. 4).

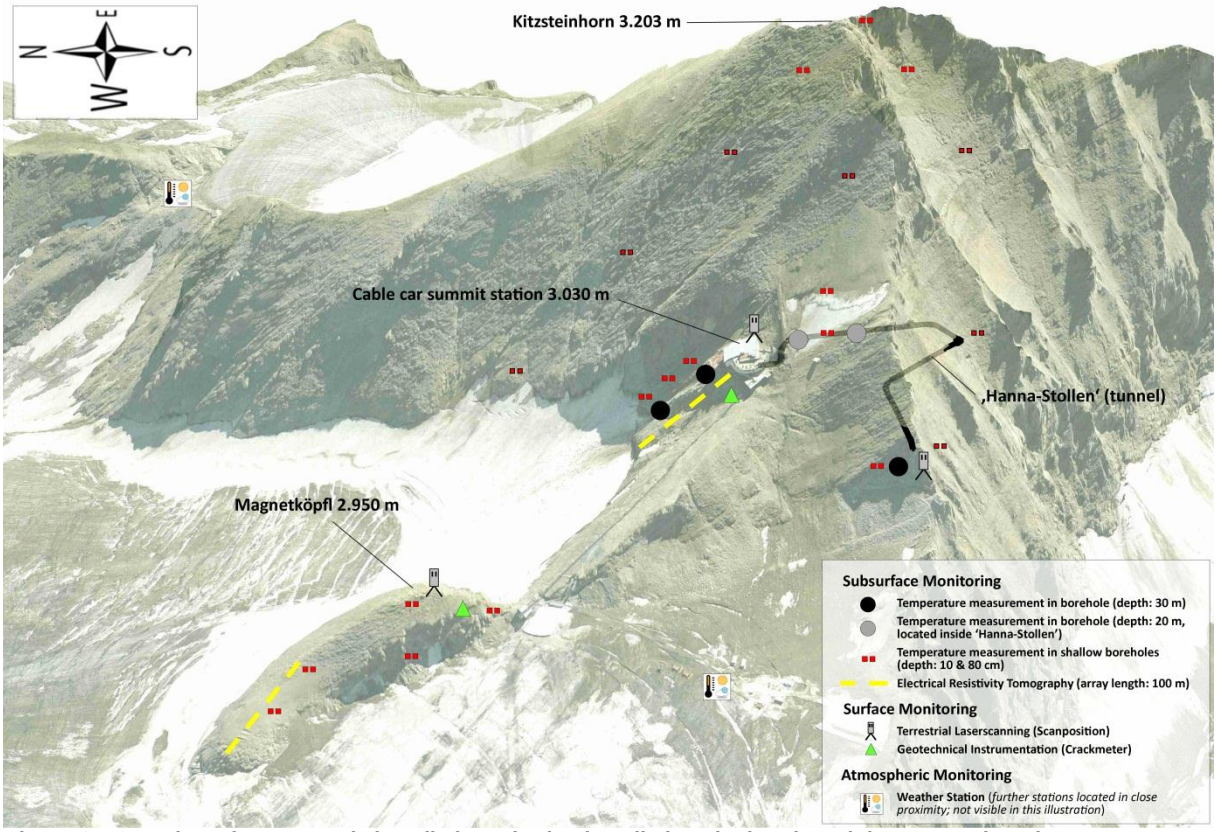

Fig. 4 - 3D-Overview of permanently installed monitoring installations in the Kitzsteinhorn summit region

Completion of the presented monitoring concept will provide a clearer image of surface and subsurface process patterns and therefore might deliver new findings on the non-trivial link between climate change and the occurrence of mass movements in steep, permafrost-affected bedrock.

Ground thermal conditions are monitored on three complementary levels (fig. 5). At each investigation level ground thermal conditions are studied applying different methodical approaches and therefore with different spatial and temporal resolutions.

- Five deep boreholes provide ground temperatures from depths of up to 30 m.
- Data from two ERT (Electrical Resistivity Tomography) arrays are used to derive information on ground temperatures.
- Spatially distributed temperature measurements with miniature loggers (iButtons) in a maximum depth of 80 cm deliver information on near-surface rock temperatures.

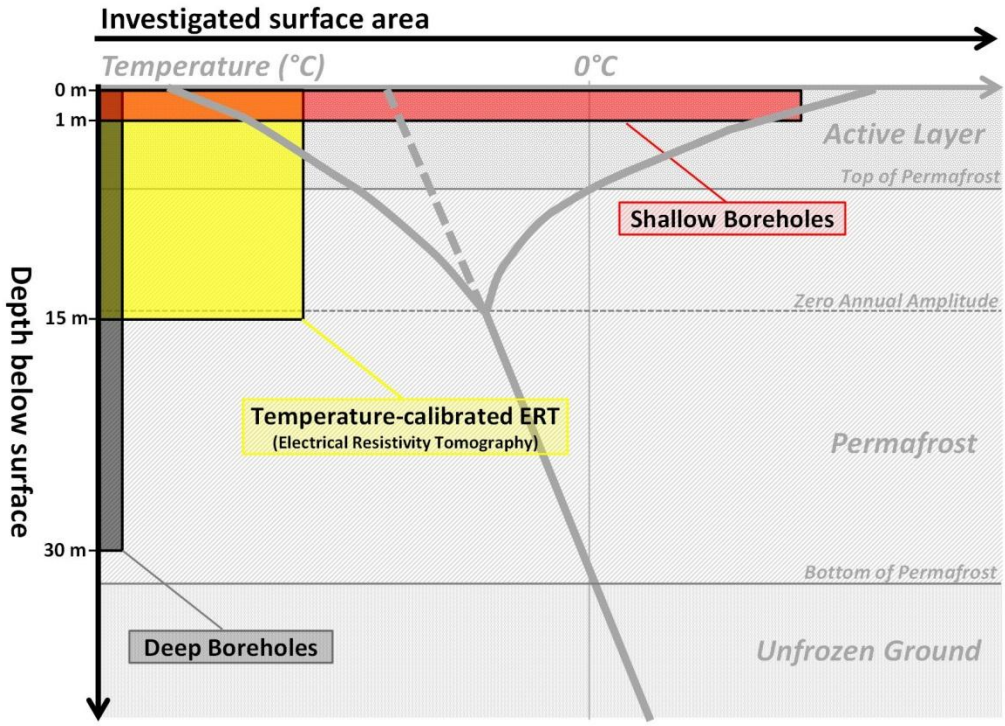

Fig. 5 - Three different methodical approaches are applied to investigate the ground thermal regime (exaggerated diagram)

2.4. Selected Results

2.4.1. Permafrost Modeling

To get a theoretical overview of the thermal state of the Kitzsteinhorn, permafrost distribution has been modeled using an advanced version of the 'Permakart' model (Version 3.0) (Keller, 1992; Schrott et al., 2012). 'Permakart 3.0' is an empirical-statistical model that calculates the probability of permafrost occurrence based on a topo-climatic key. The underlying topo-climatic key analyzes the relation between altitude, slope and aspect while also taking into account foot-slope positions.

Modeling results reveal that large areas of the Kitzsteinhorn summit pyramid are underlain by permafrost. Particularly the northwest face and to a lesser degree the northeast face display a very high probability of permafrost occurrence (> 75%). South-facing slopes show a significantly lower probability of permafrost occurrence according to the modeling results (fig. 6).

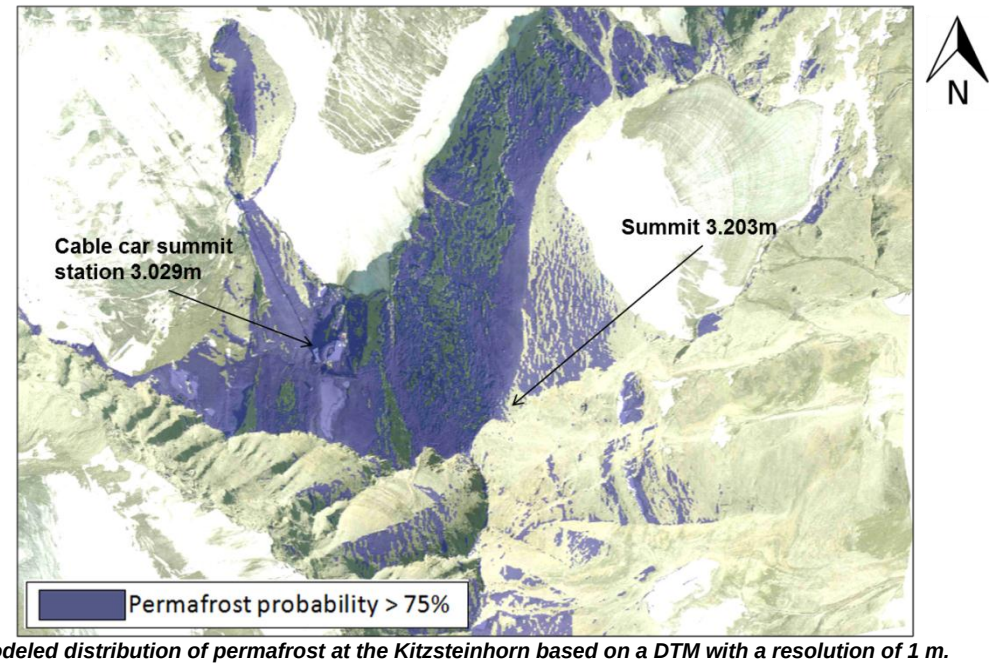

Fig. 6 - Modeled distribution of permafrost at the Kitzsteinhorn based on a DTM with a resolution of 1 m.

2.4.2. Electrical Resistivity Tomography

In order to attain first geophysical evidences of permafrost occurrence at the Kitzsteinhorn, ERT measurements have been carried out inside the 'Hanna-Stollen' (fig. 7). The 'Hanna-Stollen' connects the north side of the mountain (cable car summit station) to the south side at an altitude of approximately 3.000 m. It constitutes a cross-section through the mountain and therefore represents an intriguing opportunity to investigate the influence of aspect on permafrost occurrence along a single ERT profile line (northern vs. southern exposure).

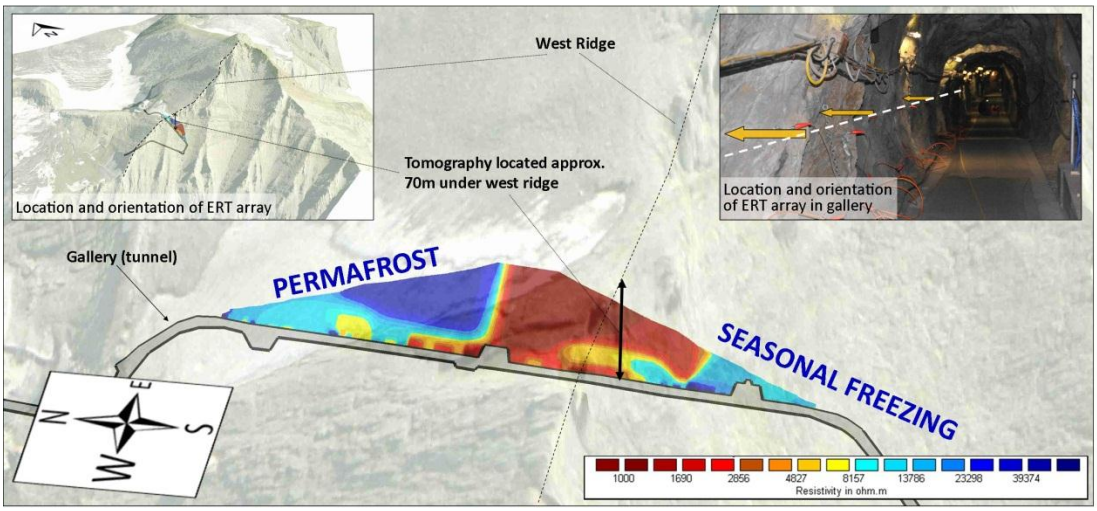

Fig. 7 - Location and orientation of ERT measurements conducted inside the 'Hanna-Stollen'.

2.4.3. Terrestrial Laserscanning

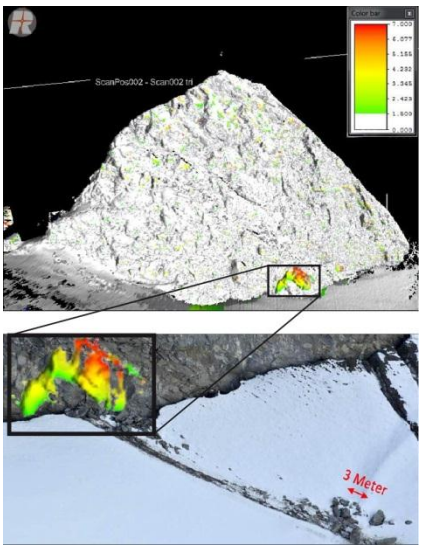

The application of TLS (terrestrial laser scanning) to detect and quantify changes occurring at the terrain surface is an integral part of the monitoring activities. In August 2011 a rock fall event directly affected a track frequently used by snow mobiles. Analysis of TLS data delivered a precise identification of the release zone and yielded a rock fall volume of approximately 140 m3 (Fig. 8). Intense lowering of the surface of the Schmiedingerkees glacier (glacial ablation) in past decades seems to be the main cause for the rock fall event.

Evaluation of weather data demonstrate that the rock fall event was preceded by pronounced warm phase. However, the actual triggering of the event happened during a cold front, which was accompanied by heavy rain. A lowering of the cohesion due to infiltrating rain water therefore might have played an important role for the triggering of the event.

Fig. 8 - Surface comparison of pre- and post-event scan (top), detachment zone and deposits of rock fall event (bottom).

2.4.4. Near-Surface Rock Temperatures

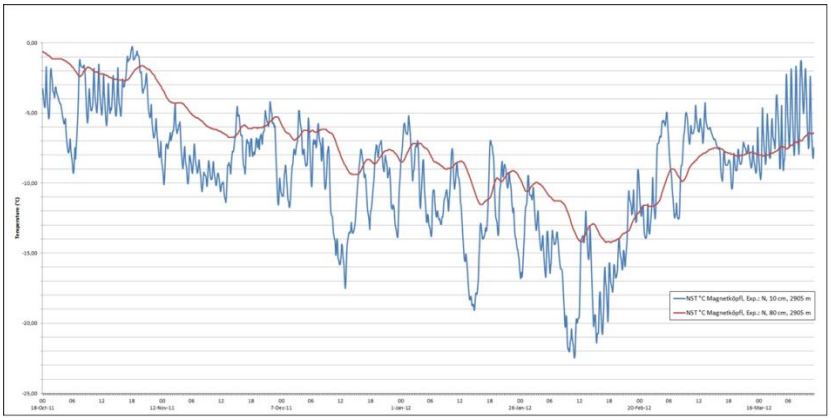

In order to resolve the spatial heterogeneity of near-surface rock temperatures, several dozens of miniature loggers (iButtons©) have been distributed across the Kitzsteinhorn summit pyramid. A special instrumentation workflow for the installation of iButtons® in depths of 10 and 80 cm was designed. First results demonstrate the applicability of the developed method.

Fig. 9 – Rock temperature in 10 cm (blue) and 80 cm depth (red).

Acknowledgements
The research project MOREXPERT ('Monitoring Expert System for Hazardous Rock Walls') is supported by numerous companies and scientific partners. The authors want to particularly thank Gletscherbahnen Kaprun AG, Geoconsult ZT GmbH, Geodata GmbH, Geolog 2000 Fuss/Hepp GdbR, University of Salzburg, University of Bonn, University of Graz, Z_GIS – Centre for Geoinformatics and the Salzburg Research GmbH for financial, material and intellectual support.

3. Proglacial dynamics at the Obersulzbachkees - Martin Geilhausen

This day focuses on geomorphic processes within the proglacial zone of the Obersulzbachkees. Data and results presented have been achieved within the SedyMONT research project (Timescales of sediment dynamics, climate and topography change in Mountain Environments, www.sedymont. sbg.ac.at) as part of the TOPO-Europe programme of the European Science Foundation.

3.1. Our research at the Obersulzbachkees

In SedyMONT, we have investigated the intensity and spatio-temporal variability of sediment transfer and paraglacial landform adjustment in two glacier forefields in the Austrian Alps. The sediment budget framework forms the conceptual basis of our study.

3.1.1. Sediment budget approach & framework

"A sediment budget for a drainage basin is a quantitative statement of the rates of production, transport and discharge of detritus." (*Dietrich et al., 1982*)

"A sediment budget is an accounting of the sources and disposition of sediment as it travels from its point of origin to its eventual exit from a drainage basin." (*Reid & Dunne, 1996*)

As such, it is a mass balance approach that provides a holistic understanding of the links between sediment production, intermediate storage, transfer and yield. *Jordan & Slaymaker* (1991) expressed that in the mathematical formula

$$\Delta S_t = I_t - O_t$$

with ΔS = storage change, I = sediment input, O = sediment output and t = time.

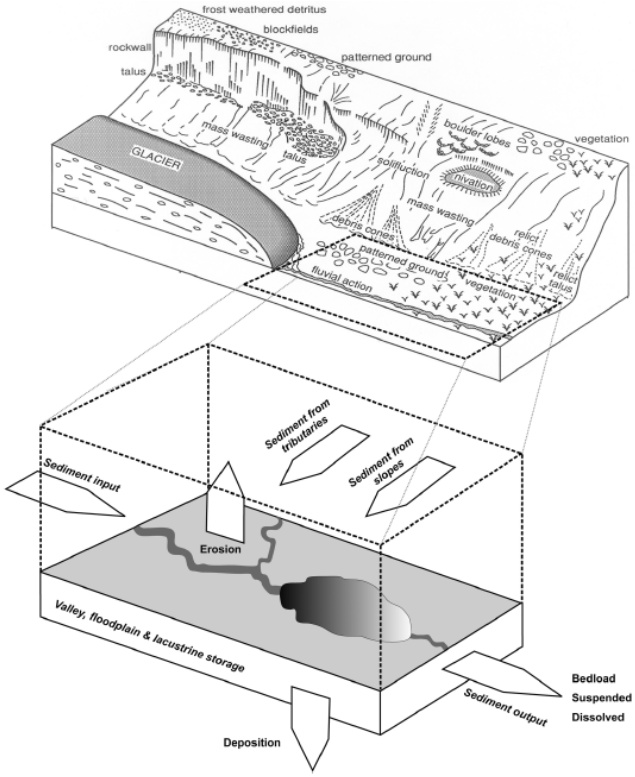

Fig. 10. - Schematic diagram of a valley glacier landsystem with characteristic processes, sediment storage units and main sediment budget components (Orwin et al., 2010).

3.1.2. Paraglacial sedimentation

"…non-glacial processes that are directly conditioned by glaciation." *(Church & Ryder, 1972)*

"The withdrawal of glacier ice exposes landscapes that are in an unstable or metastable state, and consequently liable to modification, erosion and sediment release at rates greatly exceeding background denudation rates." *(Ballantyne, 2002)*

"...non-glacial earth surface processes, sediment accumulations, landforms, landsystems and landscapes that are directly conditioned by glaciation and deglaciation." *(Ballantyne, 2002)*

From Ballantyne's enlarged definition of 'paraglacial', the fundamental question raises of how to discriminate between 'proglacial', 'periglacial' and 'paraglacial'.

"Where a landscape is paraglacial it can be characterised in terms of rate of change and trajectory of that change. It cannot be defined in relation to glaciers (as in proglacial) […]. Almost all paraglacial landscapes are transient and transitional." *(Slaymaker, 2009)*

Glacier forefields reveal a "short-lived form of paraglacial response, [...] within a few decades." *(Ballantyne, 2002)*

"Glacier forefields are landscapes in the process of recovering from disturbance and are susceptible to rapid topographic modifications within a few decades." *(Slaymaker, 2009)*

"[...] results showed that 'young' ice proximal surfaces exposed since 1977 were increasingly vulnerable to mobilization […]." (*Orwin & Smart, 2004)*

"The rapid temporal decline in surface response indicated that surface armouring or sediment exhaustion is stabilizing surfaces within decades of exposure from the LIA maximum […]." (*Orwin & Smart, 2004)*

"The full sequence of paraglacial slope adjustment (gully incision to stabilization) may occur […] within two decades." (*Mercier et al., 2009)*

"[...] plant colonization that are driven by temporal periods of deglaciation [...]. Vegetation colonization is a response to stabilization of the ground surface"

"[…] differences in the rates and the nature of plant colonization are biomarkers of paraglacial dynamics" (*Moreau et al., 2008)*

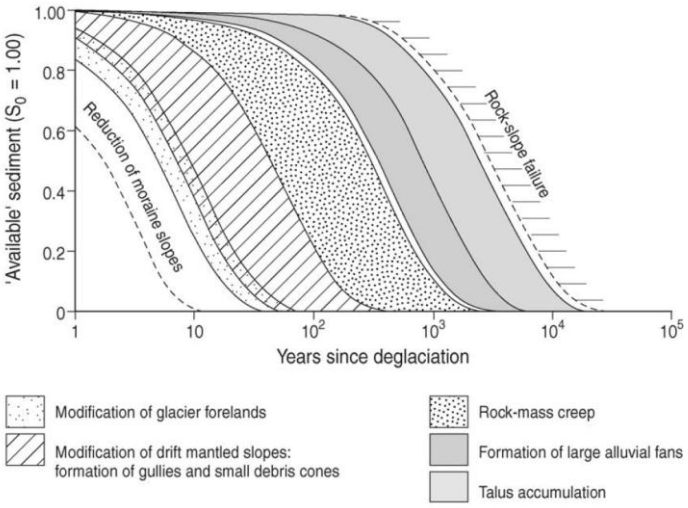

Fig. 11. - Paraglacial exhaustion curves separated by landsystem type (Ballantyne, 2002).

3.1.3. The importance of glacier forefields

Spatially, a glacier forefield extents between the LIA terminal moraine and the present glacier margin (*Kinzl, 1929*). Thus, it is an expanding zone of landform development and paraglacial adjustment due to receding glacier margins which expose fresh surfaces of unstable glacial deposits without protective vegetation cover.

Glacierized Alpine catchments and the glacier forefields therein are amongst the most dynamic geomorphic systems on planet earth and are sensitive indicators *of* and considered to be greatly impacted *by* climate change. Here, sediment budget studies are of particular importance to assess the (in)stability and sensitivity of glaciers forefield to perturbations and the sustainability of downstream land use activities (*Walling & Collins, 2008*).

For example, glacierized catchments are often used for hydropower schemes and emerging problems like increasing rates of reservoir sedimentation, that are depended on sediment flux from upstream geomorphic systems, have negative (financial) effects on the lifespan of reservoirs (*Bogen, 1989; Einsele & Hinderer, 1997*).

3.2. Overview of the Obersulzbachkees

- listed in WGMS (*WGMS 2008*), 1st reference year 1871, 1st survey year 1815, 92 observations
- nearly continuous retreat since the 'Little Ice Age' with only short periods of stability/advances in response to the cooler periods of the 1890s, 1920s and 1970s (in which the majority of Austrian glaciers advanced)
- Ø annual retreat of ca. 26 ma^{-1} in the last 6 decades resulting in a cumulative frontal retreat of ca. 1.5 km (ca. 3 km retreat since 'LIA')
- very few data on flow velocity, 1985/86 & 1986/86 in the range 4.5 - 8 ma^{-1} at the 'Türkische Zeltstadt', a former area of intensive brittle structures and crevasses at the narrow upper part of the main valley trough (*Slupetzky, 1988*)
- in the vicinity of the cable car valley station, ice thickness during the LIA was ca. 140 m
- ice thickness measurements by means of reflection seismic (7 profiles, *Brückl & Gangl, 1977*) and ground-penetrating radar (19 profiles, *Fischer et al., 2007*)

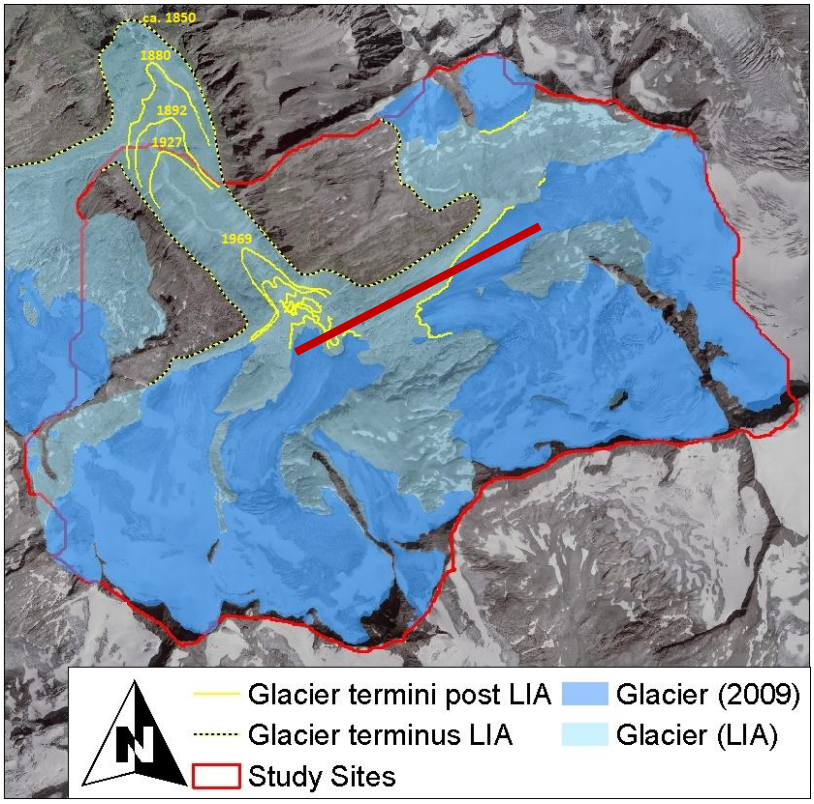

Fig. 12. - Historical to modern glacial coverage and glacier termini (pre 1969 glacier termini adopted from Slupetzky, 1986). The red line marks the seismic profile shown in figure 6.

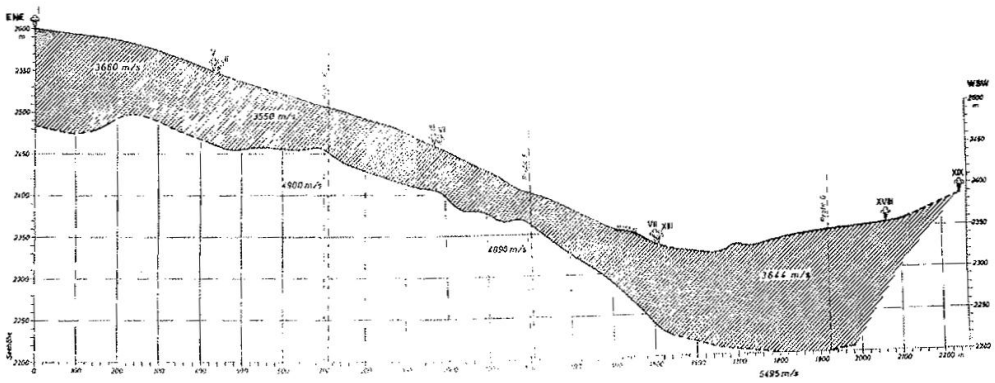

Fig. 13. - Reflection seismic survey from Brückl & Gangl (1977), for profile location see figure 3.

3.3. Sediment storage distribution at the catchment scale

- typical landform assemblage with i.) talus and scree slopes beyond the modern drift limit of the 'Little Ice Age' advance, ii.) glacigenic sediment and glacial landforms within the drift limit, iii.) glacifluvial storages in ice proximal locations and along recent and former meltwater channels, and iv.) reworked till accumulated in debris flow, avalanche and alluvial deposits at the base of incised drift mantled slopes or stream tributaries
- alpine meadows, turfs and dwarf shrubs represent the vegetation cover that extends up valley approximately as far as the 1969 glacier terminus and indicates stabilized surfaces
- moraine deposits are the dominant sediment storage type a significant source of (sub)recent sediment transfer
- paraglacial reworking is the main evolutionary factor for drift-mantled slopes with high activity in ice marginal and proximal locations (gully densities up to 3.7 per 100 metres of slope), with increasing distances to the glacier, the importance of paraglacial reworking decreases (gully density of 0.5 to 0.6)

- high degree of sediment storage activity especially in ice marginal positions demonstrates the significance of adjustment processes at the very beginning of deglaciation
- contribution of paraglacial reworking to the overall sediment output is insignificant due to decoupling effects and till and debris are currently stored in the landsystem
- spatial distribution of sediment storage types delivers a record of the historical activity of the glacier and the degree of sediment storage activity gives insights into the state of paraglacial landform adjustment

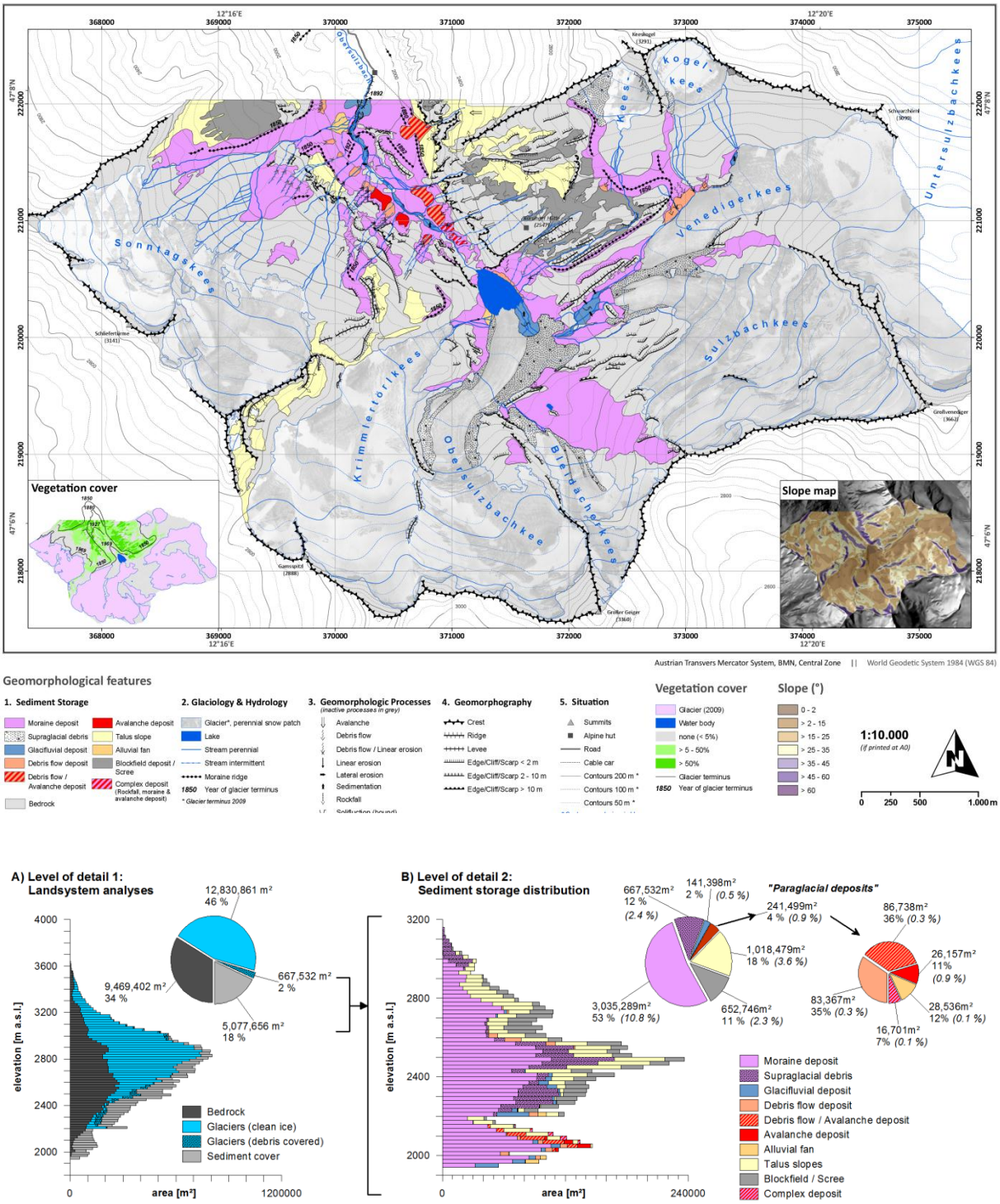

Fig. 14.- Top: Geomorphological map of the Obersulzbachkees landsystem (Geilhausen et al., 2012a). Bottom: Quantitative analyses and hypsometric distribution of glaciers, bedrock and sediment storage types at the Obersulzbachkees landsystem given in two levels of detail (LOD). LOD 1 provides a general overview of bedrock exposures, debris covered and clean ice glacier areas and total sediment coverage at the landsystem scale (plot a). LOD 2 depicts the total sediment coverage of LOD 1 in detail and gives the absolute coverage of sediment storages types and their relative contributions to the landsystem area covered by sediment (plot b). The coverage of storage types at the landsystem scale is additionally marked in brackets (Geilhausen et al. 2012a).

3.4. Overview of the development of the proglacial zone

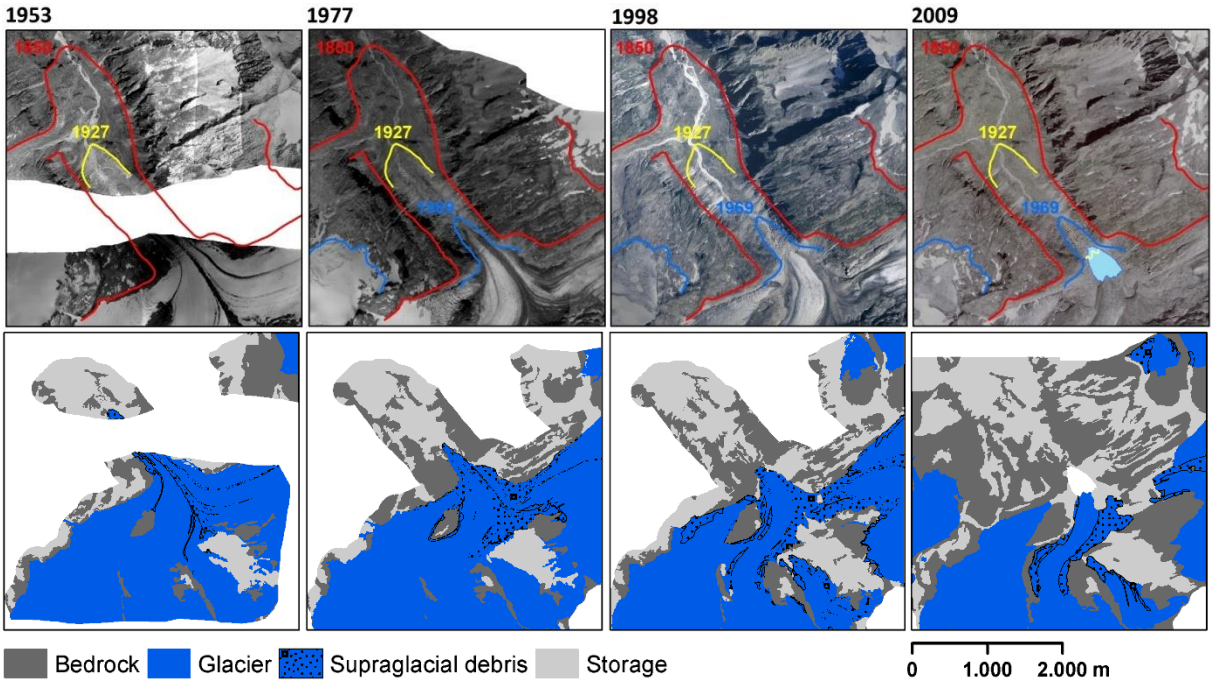

Fig. 15. - Time series maps of the development of the proglacial zone.

- since around the year 1998, the receding Obersulzbachkees has exposed a natural bedrock basin and a proglacial lake has formed that decouples coarse sediment flux from ca. 19 km² of the land-system and significantly traps suspended sediment

3.5. Sediment transfer and reworking within the proglacial zone

- multi-epoch surface comparisons (DEMs of difference) at the 68% and 95% confidence level
- DEM resolutions of 0.5m (TLS) in 2009, 2010 & 2011, and 1 m (photogrammetry) in 1953 and 1977
- sediment transfer downstream of the proglacial lake is spatially limited to a few debris flows and tributary channels
- decoupled hillslopes
- surface elevation changes 2009 - 2011 are in the range -6.5 to +5.8 m
- volume-to-mass conversion using a density of 2 ±0.25 t/m³

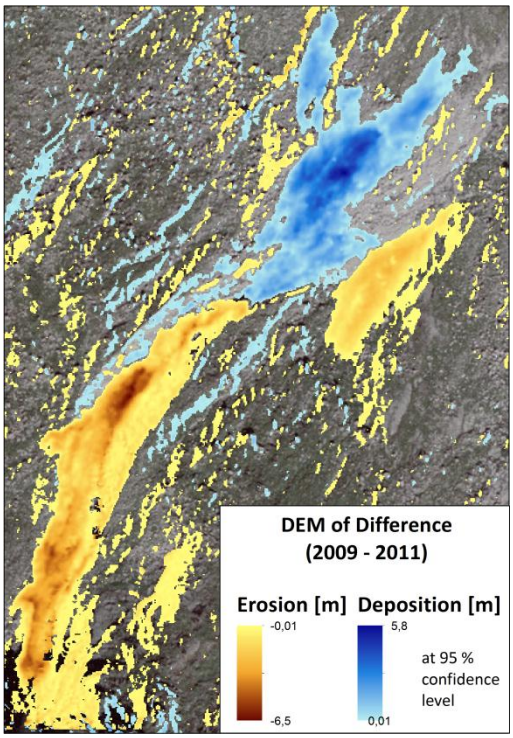

Fig. 16. - Example of DEM of difference calculation in the lower proglacial area at the 95% confidence level.

3.6. Sediment thickness and radiocarbon dating

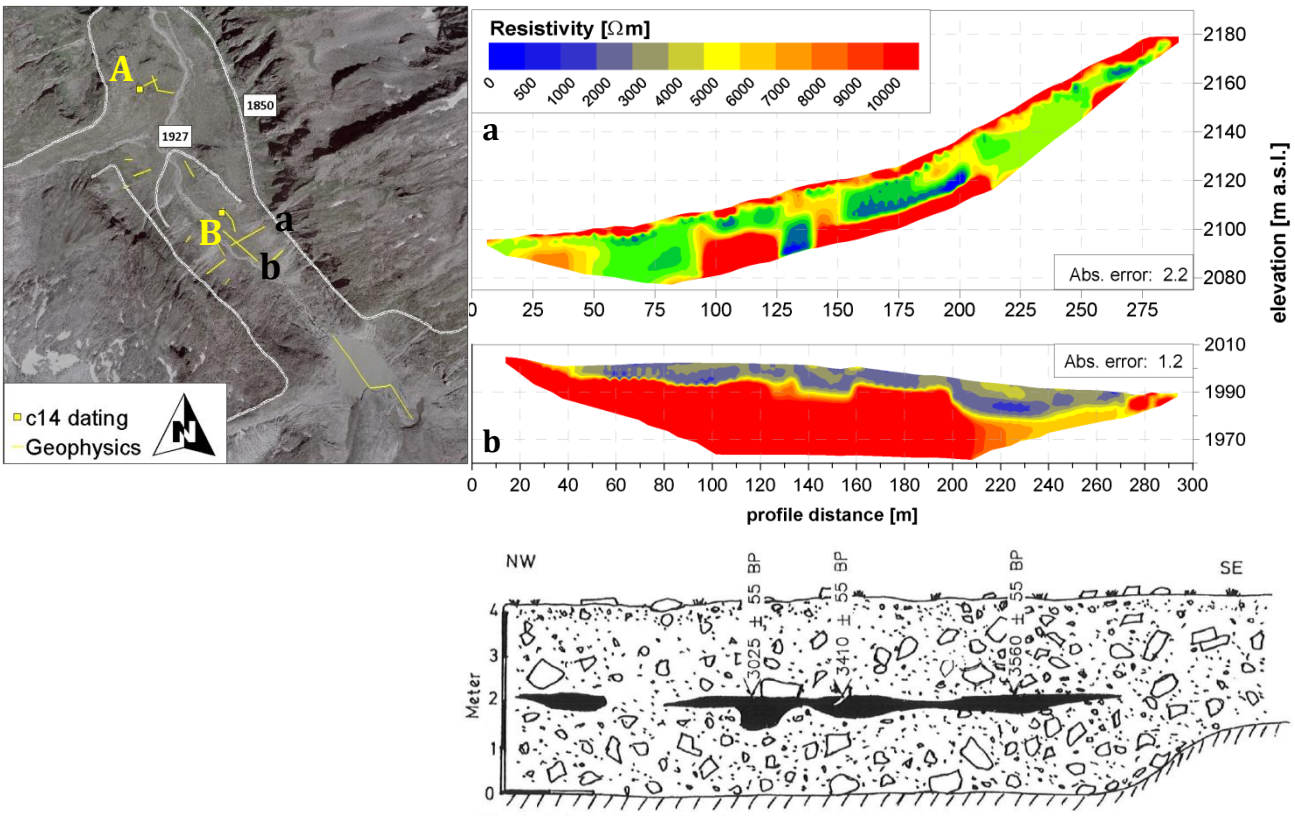

Fig. 17. - Location of geophysical profiles and ^{14}C datings (left), longitudinal and cross 2d resistivity section (upper right) and detailed sketch of a peat layer (lower right, ^{14}C sample B, from Slupetzky, 1988).

- resistivity of bedrock > 5000 Om, calibrated in field and lab
- sediment thickness: 5 – 15 m
- many bedrock outcrops in the valley favour a morphometric approach supported by geophysical surveys to model sediment thickness within the proglacial zone

- two published 14C datings (*Slupetzky, 1988*):
  - A) pinus trunk: 1620 cal. BP - pinus trunk overridden by advancing glacier, covered by glacial and glacifluvial deposits, trunk ca. 60 cm diameter and an age of 200 years based on dendrochronology
  - B) peat layer: 3560 cal. BP - compressed peat layer of max. 60 cm thickness in 2 - 2.5 m depth

- sample B is in great agreement with the 'Löbbenschwankung' advancing period 3500 – 3000 cal. BP (*Patzelt & Bortenschlager, 1973*)
- samples and data indicate that the glacier advanced over a sediment bed during LIA times, thus a certain fraction of the sediment volume currently stored in the glacier forefield is much older than 1850 (organic material has also been found in many other glacier forefields, e.g. at the Pasterze)
- *Nicolussi & Patzelt (2000)* speculated that the glacial coverage during 'Löbbenschwankung' even exceeded the LIA extent within the Venediger Range

3.7. Sediment yield from the proglacial zone

3.7.1. Suspended sediment concentrations, discharge relationships, turbidity and grain sizes

- 2010: 96.4 - 381.8 mg/l, Ø 170.2 ± 54.8 mg/l (n = 125), D_{50}: 3.02 - 7.41 µm, n = 18
- 2011: 71.3 - 702.3 mg/l, Ø 188 ± 94.1 mg/l (n = 235), D_{50}: 4.46 - 9.19 µm, n = 36
- SSC measured downstream the lake are low as compared to other proglacial environments with Ø SSC often > 1000mg/l
- strong correlations of SSC with Q, but different slopes of log-transformed SSC vs. Q regressions indicate variable sensitivities of SSC to changes in Q
- strong correlation of turbidity with SSC, turbidity strongly determined by the quantity of finer particles in suspension, particles finer 7.8 µm (r^2 = 0.756, p < 0.001), half phi classes of 2 - 3.9 µm and > 3.9 - 5.5 µm are of mayor importance (r^2 = 0.747, p < 0.001)

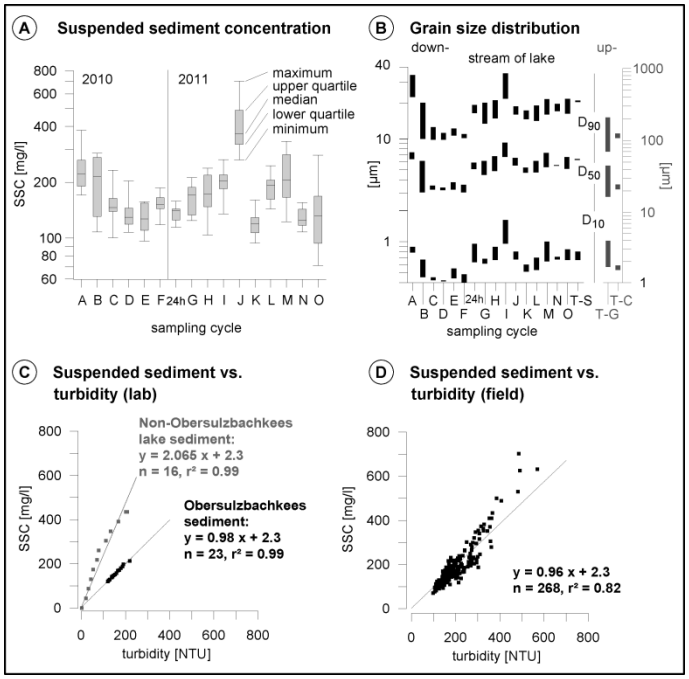

Fig. 18. - Suspended sediment concentrations (A), corresponding grain size distributions (B), turbidity vs. SSC rating curves (C & D, Geilhausen et al. 2012b).

3.7.2. Solute concentrations, discharge relationships and electrical conductivity

- 3.58 to 8.33 mg/l, Ø 5.56 mg/l (n = 45), also considered to be low
- Ø SOC of 1.18 mg/l from snow samples used for atmospheric correction
- strong correlations of SOC with Q and electrical conductivity

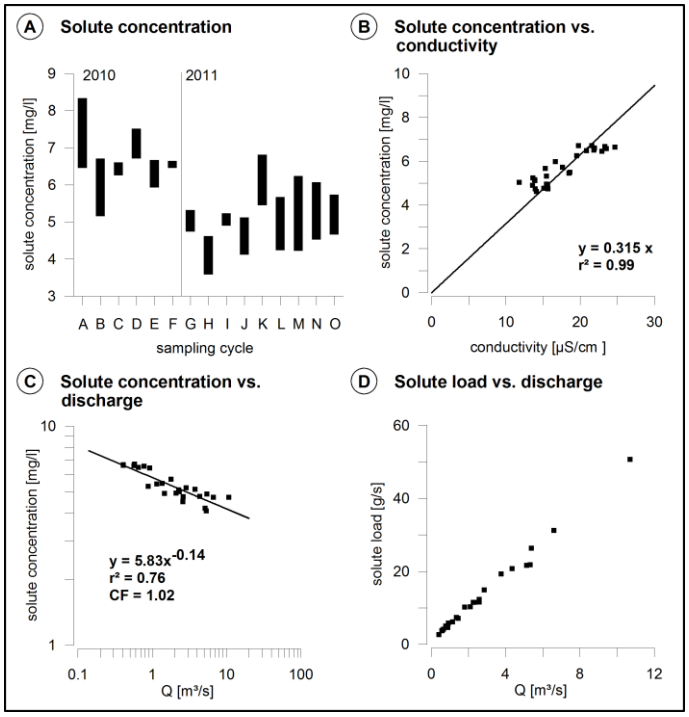

Fig. 19. - Solute concentrations (A), solute concentrations vs. conductivity relationship (B), solute concentration - discharge rating curve (C) and solute load vs. discharge relations ship (D, Geilhausen et al. 2012b).

3.7.3. Calculation of suspended sediment & solute loads

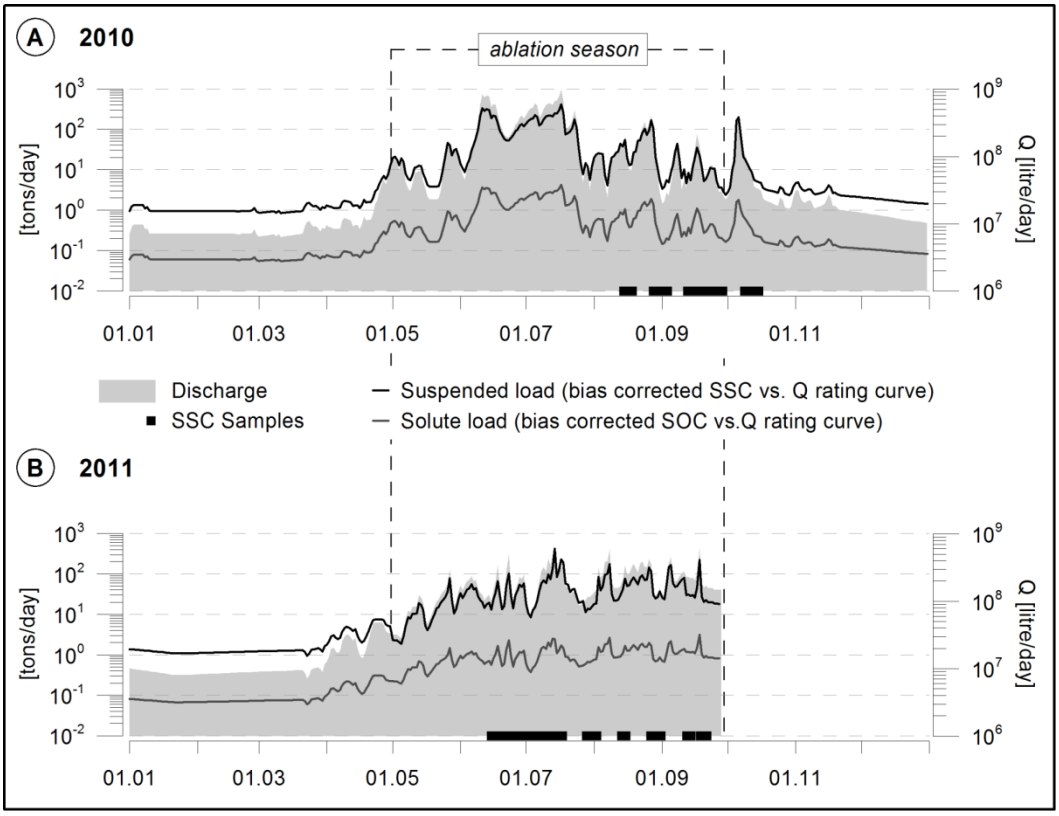

Fig. 20. - Bias corrected daily suspended sediment and solute loads, both depicted in tons per day and discharge displayed in litres in 2010 (A) and 2011 (B). Note that both axes of ordinates are log scaled. Suspended sediment loads exceed solute loads in general by at least 1 to 1.5 orders of magnitude (Geilhausen et al. 2012b).

- 15 min. concentrations predicted by i.) the rating curve method and ii.) 15 min. turbidity and conductivity records
- bias correction factor [CF = exp(2.651*S²] to overcome load underestimation applied (*Ferguson, 1986*), S² calculated using residual sum of squares (RSS) divided by number of degrees of freedom (n-2)
- **suspended load: 17826 ± 192 t (*Tu*) 18052 ± 210 t (*Qr*)**
- **solute load: 344 ± 2.2 t (*EC*)** 347 ± 2.2 t (*Qr*) **265 - 269 ± 1.7 t (*corrected*)**
- **total load: 18170 ± 194 t (*Qr*) 18399 ± 212 t (*sensor)***
- **Ø annual specific sediment yield (SSY) in the range of 451 ± 5 t/km²/a - 457 ± 5 t/km²/a**
- suspended load accounts for 98 %, ca. 77 % of solute load probably originate from chemical weathering
- 94 % of total load exported in the ablation seasons

3.7.4. Bed load

- lake decouples ca. 19 km² and leads to sediment deficient flow ('hungry water', *Kondolf 1997*)
- single thread channel and decoupled hillslopes downstream of the lake
- exploitation of bed load sources to limited to channel bed, bar & bank erosion
- reaches, bars and banks are stable and mostly vegetated, often boulder-armoured and fine sediment has already been winnowed away
- **interrupted and supply limited present day bed load transport system, we hypothesize that bed load has been low during the duration at least within the duration of monitoring (20 month)**

3.8. How the proglacial zone takes control on sediment yield

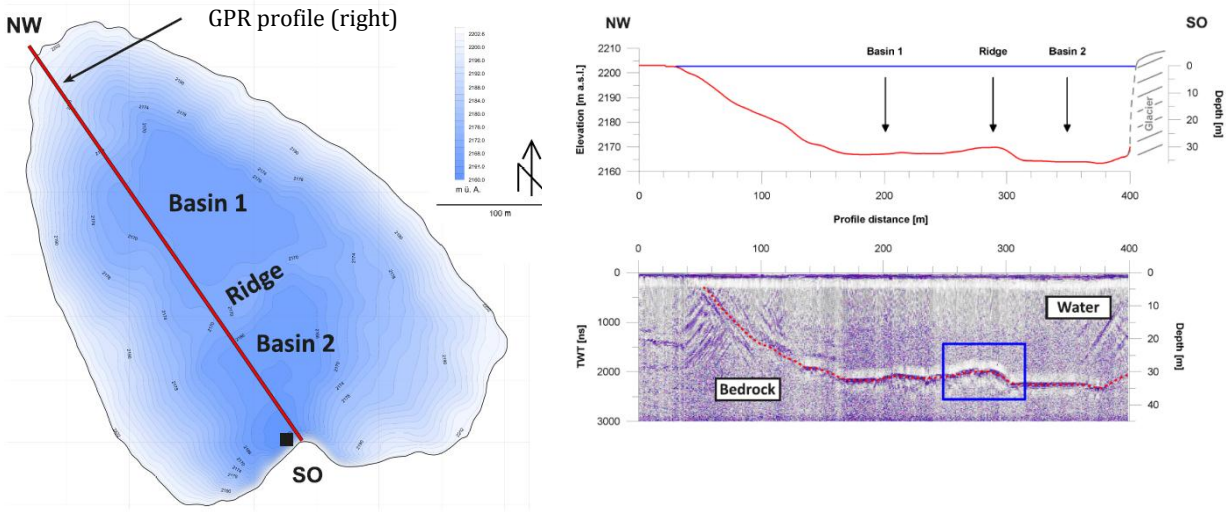

Fig. 21. - Bathymetry of the proglacial lake (left, Kum 2010, data provided by the Hydrographical Service of the Province of Salzburg) and GPR survey and interpretation (right).

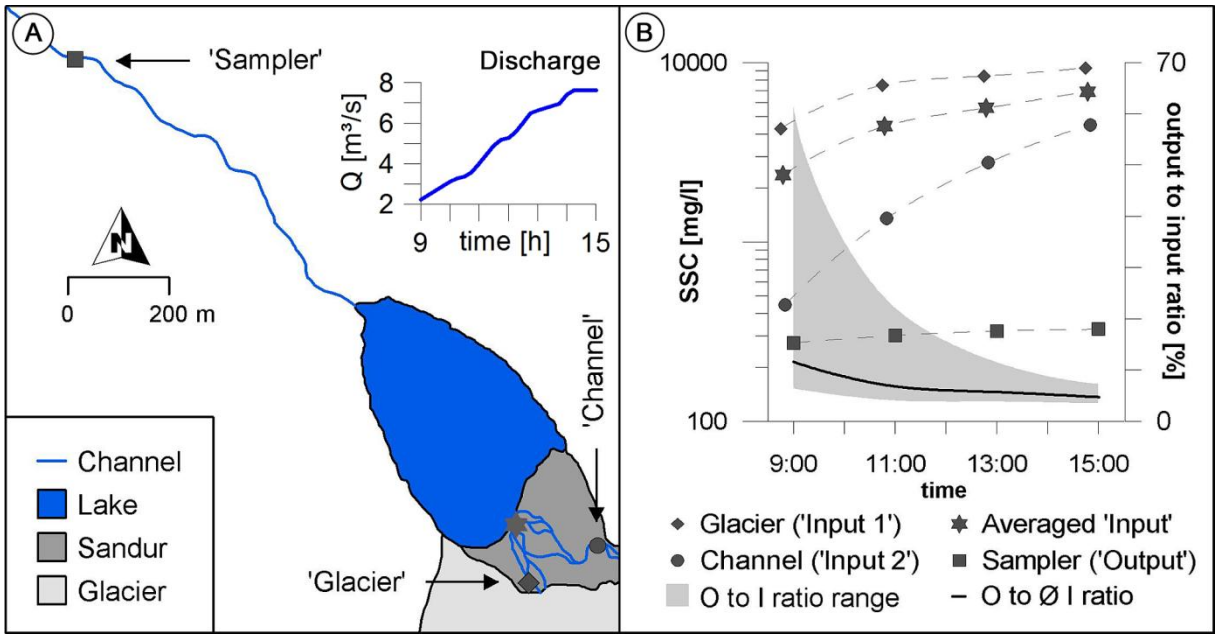

Fig. 22. - Set up of a synchronous sampling experiment carried out August 26th 2011, samples at 'Glacier' and 'Channel' location were taken manually ~ 10 min prior to the automated sampling at the monitoring site 'Sampler' every 2 hours from 09:00 to 15:00 at discharge ranging from 2.2 - 7.6 m³/s (Geilhausen et al. 2012b).

- maximum depth of ~ 42.4 m directly in front of the glacier, lake floor characterized by steep slope gradients to a depth of 30 m, two nearly plain basins located in the central part dissected by a distinct ridge of 6-7 m
- radar patterns of the ridge indicate sediment structures and are interpreted as a moraine ridge dumped and/or pushed between 2003 and 2006
- the lake damps suspended sediment concentrations by 88 - 95 % with a corresponding reduction of particle sizes to the fraction of fine to middle silt

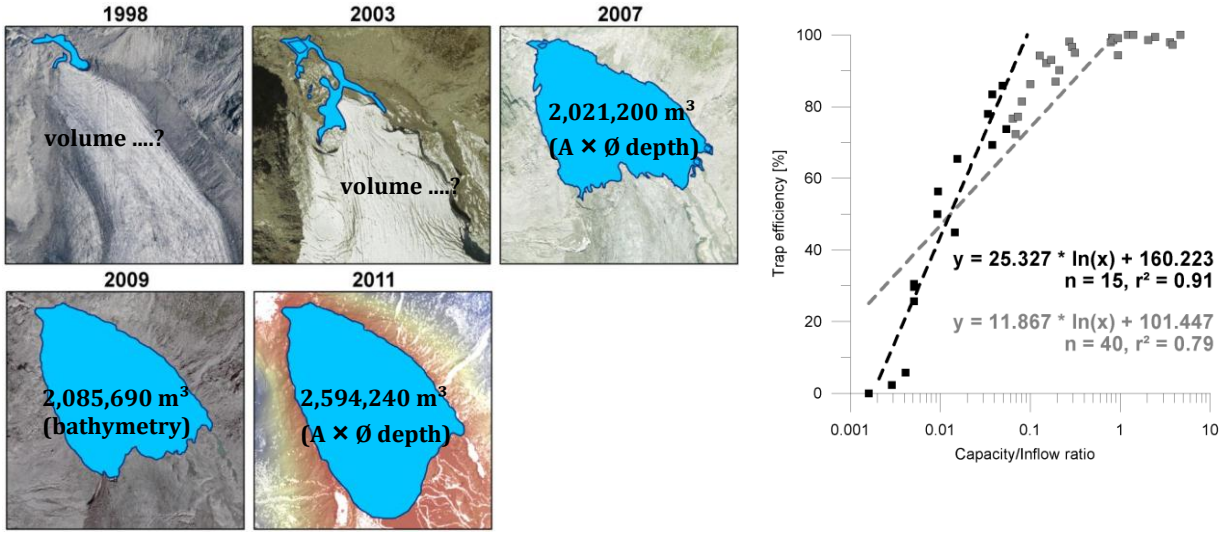

Fig. 23. - Time series maps of proglacial lake development (left) and statistical relationship of capacity/inflow ratio and trap efficiency (modified from Brune, 1953).

- we have used the capacity/inflow ratio *(Brune, 1953)* for trap efficiency back-calculation to extend suspended sediment loads to the time period of available discharge data (1989)
- **min. SSL exported since 1989 in the order of 30 .2 × 10^4 t** (Ø SSC × Q, the output from the lake is assumed to be constant)
- trap efficiency estimation of ~ 90% in 2011 (field data), 76 % in 2009 (0.036 C/I - ratio), and 82 % in 2007 (0.046 C/I - ratio), however, we have limited data on lake volume and thus on the C/I - ratio in the period of 1998 - 2007
- as there was no lake prior to 1998, SSL correction is computed by:

$$SSL_{cor(t)} = SSL_{cal(t)} \times (1 + (1\text{-}TE_{(t)}))$$

- **estimated SSL_{cor} since 1989: ~ 43 × 10^4 t**

Acknowledgements: The study presented is part of an individual project of the University of Salzburg within the collaborative research project SedyMONT (Timescales of Sediment Dynamics, Climate and Topographic Change in Mountain Environments, ESF TOPO-EUROPE programme, www.sedymont.sbg.ac.at). Financial funding by the Austrian Science Fund (FWF): Projektnummer I 157-N19 is gratefully acknowledged.

References

Ballantyne, C.K. (2002): Paraglacial geomorphology. Quaternary Science Reviews 21: 1935-2017.

Bogen, J. (1989): Glacial sediment production and development of hydro-electric power in glacierized areas. Ann. Glaciol. 13: 6-11.

Brückl, E. & Gangl, G. (1977): Seismic and dynamic investigations of glaciers in the Venediger group (Obersulzbachkees and Untersulzbachkees, Austria). Transactions-American Geophysical Union 58(9): 902-902.

Brune, G. (1953): Trap efficiency of reservories. Trans AGU 34(3): 407-418.

Church, M. & Ryder, J.M. (1972): Paraglacial sedimentation: a consideration of fluvial processes conditioned by glaciation. Geol. Soc. Am. Bull. 83: 3059-3071.

Davies, M. C. R., O. Hamza, B. W. Lumsden, & C. Harris (2000): Laboratory measurements of the shear strength of ice-filled rock joints, Ann. Glaciol., 31, 463–467, doi:10.3189/172756400781819897.

Dietrich, W.E., Dunne, T., Humphrey, N.F. & Reid, L.M. (1982): Construction of sediment budgets for drainage basins. - In: F.J. Swanson, R.J. Janda, T. Dunne & Swanson, D.N. (eds.), Sediment Budgets and Routing in Forested Drainage Basins. United States Department Agriculture Forest Service: 5-23.

Einsele, G. & Hinderer, M. (1997): Terrestrial sediment yield and the lifetimes of reservoirs, lakes, and larger basins. Geologische Rundschau 86 (2): 288-310.

Ferguson, R.I. (1986): River loads underestimated by rating curves. Water Resources Research 22: 74-76.

Finger, F., Frasl, G., Haunschmid, B., Lettner, H., von Quadt, A., Schermaier, A., Schindlmayr, A.O. & Steyrer, H. P. (1993): The Zentralneise of the Tauern Window (Eastern Alps): Insight into an Intra-Alpine Variscan Batholith. In: von Raumer, J. F und Neubauer, F. (eds.) – Pre-Mesozoic Geology in the Alps. Springer (Berlin. Heidelberg, New York) 1993, 375-391.

Fischer, A., Span, N., Kuhn, M. & Butschek, M. (2007): Radarmessungen der Eisdicke österreichischer Gletscher. Band II: Messungen 1999 bis 2006. Österreichische Beiträge zu Meteorologie und Geophysik 39.

Geilhausen, M., Otto, J.-C. & L. Schrott (2012a): Spatial distribution of sediment storage types in two glacier landsystems (Pasterze & Obersulzbachkees, Hohe Tauern, Austria). Journal of Maps (http://dx.doi.org/10.1080/17445647.2012.708540).

Geilhausen, M., Morche, D., Otto, J.-C. & L. Schrott (2012b): Sediment discharge from the proglacial zone of a retreating Alpine glacier (Obersulzbachkees, Hohe Tauern, Austria). Zeitschrift für Geomorphologie.In press.

Hartmeyer, I., Keuschnig, M., Delleske, R. and Schrott, L., 2012. Reconstruction of the Magnetköpfl event - Detecting rock fall release zones using terrestrial laser scanning, Hohe Tauern, Austria. Geophysical Research Abstracts, Vol. 14, EGU2012-12488.

Gruber, S. & Haeberli, W. (2007): Permafrost in steep bedrock slopes and its temperature-related destabilization following climate change. Journal of Geophysical Research, 112, F02S13, doi:10.1029/2006JF000547.

Harris, C., Haeberli, W., Vonder Muehll, D. & King, L. (2001): Permafrost Monitoring in the High Mountains of Europe: the PACE Project in its Global Context. Permafrost and Periglacial Processes, 12, 3–11.

Jordan, P. & Slaymaker, O. (1991): Holocene sediment production in Lillooet river basin, British Columbia: a sediment budget approach. Géographie Physique et Quaternaire 45 (1): 45-57.

Keller, F. (1992): Automated mapping of mountain permafrost using the program PERMAKART within the geographical information system ARC/INFO. Permafrost and Periglacial Processes, 3, 133-138.

Keuschnig, M., Hartmeyer, I., Otto, J.-C. & Schrott, L. (2011): A new permafrost and mass 550 movement monitoring test site in the Eastern Alps – Concept and first results of the MOREXPERT project. Managing Alpine Future II – Inspire and drive sustainable mountain regions. Proceedings of the Innsbruck Conference, November 21-23, 2011. (= IGF-Forschungsberichte 4). Verlag der Österreichischen Akademie der Wissenschaften: Wien.

Kinzl, H. (1929): Beiträge zur Geschichte der Gletscherschwankungen in den Ostalpen. Zeitschrift für Gletscherkunde für Eiszeitenforschung und Geschichte des Klimas 17: 66-121.

Klee, A. & Riedl, C. (2011): Case studies in the European Alps – Hoher Sonnblick, Central Austrian Alps. In: Kellerer-Pirklbauer, A., Lieb, G. K., Schoeneich, P., Deline, P., and Pogliotti, 560 P. (eds): Thermal and geomorphic permafrost response to present and future climate change in the European Alps. PermaNET project, final report of Action 5.3., 59-65.

Kondolf, G.M. (1997): Hungry water: Effects of dams and gravel mining on river channels. Environmental Management 21(4): 533-551.

Krautblatter, M., Verleysdonk, S., Flores-Orozco, A. & A. Kemna (2010): Temperature-calibrated imaging of seasonal changes in permafrost rock walls by quantitative electrical resistivity tomography (Zugspitze, German/Austrian Alps). Journal of Geophysical Research, 115, F02003, doi:10.1029/2008JF001209.

Kum, G. (2010): Vermessung Obersulzbachsee. Bericht-Nr. 09/023-B01. DWS Hydro-Ökologie GmbH, Wien. Unpublished technical report.

Mair, V., Zischg, A., Lang, K., Tonidandel, D., Krainer, K., Kellerer-Pirklbauer, A., Deline, P., Schoeneich, P., Cremonese, E., Pogliotti, P., Gruber, S. and Böckli, L. (2011): PermaNET - Permafrost Long-term Monitoring Network. Synthesis report. INTERPRAEVENT Journal series 1, Report 3. Klagenfurt.

Mellor, M. (1973): Mechanical properties of rocks at low temperatures, paper presented at 2nd International Conference on Permafrost, Int. Permafrost Assoc., Yakutsk, Russia.

Mercier, D., Etienne, S., Sellier, D., & Andre, M. F. (2009): Paraglacial gullying of sediment-mantled slopes: a case study of Colletthogda, Kongsfjorden area, West Spitsbergen (Svalbard). Earth Surface Processes and Landforms 34(13): 1772-1789.

Moreau, M., Mercier, D., Laffly, D. & Roussel, E. (2008): Impacts of recent paraglacial dynamics on plant colonization: A case study on Midtre Lovenbreen foreland, Spitsbergen (79 degrees N). Geomorphology 95(1-2): 48-60.

Noetzli, J. & Vonder Muehll, D. (eds.) (2010): Permafrost in Switzerland 2006/2007 and 2007/2008., Glaciological Report (Permafrost) No. 8/9 of the Cryospheric Commission of the Swiss Academy of Sciences, 68 pp.

Nicolussi, K. & G. Patzelt (2000): Discovery of early-Holocene wood and peat on the forfield of the Pasterze Glacier, Eastern Alps, Austria. The Holocene 10(2): 191-199.

Orwin, J.F., Lamoureux, S.F., Warburton, J. & Beylich, A. (2010): Framework for characterizing fluvial sediment fluxes from source to sink in cold environments. Geografiska Annaler 92A(2): 155-176.

Orwin, J.F. & Smart, C.C. (2004): The evidence for paraglacial sedimentation and its temporal scale in the deglacierizing basin of Small River Glacier, Canada. Geomorphology 58 (1-4): 175-202.

Patzelt, G. & Bortenschlager, S. (1973): Die postglazialen Gletscher- und Klimaschwankungen in der Venediger Gruppe (Hohe Tauern, Ostalpen). Zeitschrift für Geomorphologie N.F. Suppl. 16: 25-72.

Reid, L.M. & Dunne, T. (1996): Rapid evaluation of sediment budgets. GeoEcology paperback. Catena Verlag, (GeoScience Publisher), Reiskirchen, 164 pp.

Schrott, L., Otto, J.-C., Keller, F. & Rosner, M.-L. (2012): Permafrost in den Hohen Tauern. Abschlussbericht des Permalp Projektes. Universität Salzburg, 33 pp (unpublished).

Slaymaker, O. (2009): Proglacial, periglacial or paraglacial. Periglacial and Paraglacial Processes and Environments. J. Knight & S. Harrison. London, The Geological Society Special Publications 320: 71-84.

Slupetzky, H. (1988): Radiokarbon-Datierungen aus dem Vorfeld des Obersulzbachkees, Venediger Gruppe, Hohe Tauern. Zeitschrift für Gletscherkunde und Glazialgeologie 24(2): 161-165

Slupetzky, H. (1986): Gletscherweg Obersulzbachtal. Naturkundlicher Führer zum National Park Hohe Tauern, Band 4, Oesterreichischer Alpenverein, Innsbruck.

Walling, D. & Collins, A. (2008): The catchment sediment budget as a management tool, Environmental Science and Policy 11: 136-143.

WGMS (2008): Global Glacier Changes: facts and figures. Zemp, M., Roer, I., Kääb, A., Hoelzle, M., Paul, F. and Haeberli, W. (eds.), UNEP, World Glacier Monitoring Service, Zurich, Switzerland. 88pp.